

Sensing Performance of Efficient Cyclostationary Detector with Multiple Antennas in Multipath Fading and Lognormal Shadowing Environments

Ying Zhu, Jia Liu, Zhiyong Feng, and Ping Zhang

Abstract: Spectrum sensing is a key technical challenge for cognitive radio (CR). It is well known that multicycle cyclostationarity (MC) detection is a powerful method for spectrum sensing. However, a conventional MC detector is difficult to implement because of its high computational complexity. This paper considers reducing computational complexity by simplifying the test statistic of a conventional MC detector. On the basis of this simplification process, an improved MC detector is proposed. Compared with the conventional detector, the proposed detector has low-computational complexity and high-accuracy sensing performance. Subsequently, the sensing performance is further investigated for the cases of Rayleigh, Nakagami- m , Rician, and Rayleigh fading and lognormal shadowing channels. Furthermore, square-law combining (SLC) is introduced to improve the detection capability in fading and shadowing environments. The corresponding closed-form expressions of average detection probability are derived for each case by the moment generation function (MGF) and contour integral approaches. Finally, illustrative and analytical results show the efficiency and reliability of the proposed detector and the improvement in sensing performance by SLC in multipath fading and lognormal shadowing environments.

Index Terms: Improved MC detector, MGF, Nakagami- m fading, Rayleigh fading, Rayleigh fading and lognormal shadowing, Rician fading, SLC, spectrum sensing.

I. INTRODUCTION

With the rapid growth of wireless communications, the available spectrum is becoming overcrowded. To alleviate the spectrum shortage problem, cognitive radio (CR) was first introduced by Mitola in 1999 [1] and provides a way to use the valuable radio spectrum in an efficient manner. These radios are actually unlicensed wireless devices that temporarily utilize the unused primary spectral bands [2]–[4]. However, the first step in opportunistic access to the licensed spectrum is the detection of unused spectral bands [5]–[7]. In addition, CR should vacate the primary spectral band as soon as a primary user (PU) starts transmitting. Briefly speaking, spectrum sensing and transmission opportunity exploitation are the main challenges to CR networks.

Manuscript received September 15, 2013.

Y. Zhu is with the Key Laboratory of Universal Wireless Communications, Ministry of Education, Beijing University of Posts and Telecommunications, Beijing, P.R.China and Department of Teaching and Practicing, Guilin University of Electronic Technology, Guilin, P.R.China, email: zhuyingbupt@gmail.com.

J. Liu, Z. Feng, and P. Zhang are with the Key Laboratory of Universal Wireless Communications, Ministry of Education, Beijing University of Posts and Telecommunications, Beijing, P.R.China.

Digital object identifier 10.1109/JCN.2014.000027

Different approaches for spectrum sensing for CR applications have been proposed [8]–[11]. The commonly considered approaches are based on power spectrum estimation, energy detection, and multicycle cyclostationary (MC) detection. Power spectrum estimation may not function reliably in a regime with a low signal-to-noise ratio (SNR). Energy detection, on the other hand, is subject to uncertainty in noise and interference statistics. MC detection, which uses inherent properties of digital modulated signals, has been proposed in the literature to overcome the above problems [11]–[13]. In fact, it is well known that if a signal has strong cyclostationary properties, it can be detected at low SNRs. In addition, MC detector can inherently distinguish PUs from secondary users as well as interferers if they have dissimilar cyclic features [23].

Although conventional MC detectors operate significantly better than energy and power detectors, they require extensive computation to provide sufficiently low error probability, which causes high computational complexity [12], [13]. High computational complexity leads to a long detection time, which seriously degrades the spectrum efficiency of the CRs because all communications should be stopped during detection. Many papers focus on reducing the computational complexity of conventional MC detectors. In [14], a cooperative MC detector was proposed in which the detector combines distinct single-cycle (SC) detectors for different cycle frequencies (CFs), and the final decision is obtained by an OR rule (a hard decision rule for cooperative sensing) and the primitive decisions of the SC detectors. An adaptive cooperative cyclostationary beamforming-based spectrum sensing method with affordable complexity was introduced for multiple-antenna CR in [15]. In [16], a sequential framework was proposed for a collaborative MC detector in order to reduce the average detection time. In [17]–[19], cooperative cyclostationary methods were proposed to improve performance. The cooperative and collaborative MC detectors above were both introduced to reduce computational complexity. In the proposed cooperative and collaborative schemes, the computation of test statistics is performed by a group of cooperative CRs in a distributed manner such that the complexity burden on a single CR is reduced. Nevertheless, a major drawback of these schemes is the need for a very large number of cooperative CRs to make MC detection reliable, which is sometimes impractical in a CR system. Therefore, it is still necessary to improve the conventional MC detector for single CR in a local spectrum sensing scheme.

Furthermore, because the channel from the PU to the CR is multipath fading and shadowing in practical CR networks, the signal of the PU might be severely attenuated before it reaches

the CR [20]. That is to say, the analysis of sensing performance over fading and shadowing channels could help quantify the exact sensing performance of a detector. However, the existing studies are mainly restricted to Rayleigh fading, which is not sufficiently comprehensive [21], [22]. To our best knowledge, none of the previous work has addressed the issue of a MC detector over Nakagami-m and Rician fading channels. Despite focus on the sensing performance over fading channels, all the previous studies have omitted the effect of shadowing. In a practical implementation, many detectors will be found either in stationary positions or with low mobility in an environment with a varying degree of vegetation cover [23]. This foliage and the temporal stationary behaviors introduce another degradation known as shadowing, which cannot be mitigated by averaging the received signal strength [24]. Hence, if we wish to examine the exact sensing performance of an MC detector, the effect of shadowing needs to be investigated.

Moreover, multiple antennas for spectrum sensing can be deployed to improve the sensing performance in severe fading and shadowing conditions [22], [25]. The need for multiple antennas is also driven by the promise of a high data rate and high-efficiency broadband services by standards such as long term evolution (LTE), worldwide interoperability for microwave access (WiMax), and international mobile telecommunications-advanced (IMT-Advanced). The notion of using a multiple-antenna CR for detecting the spectrum holes has thus attracted significant interest. In [22] and [25], the linear combinations of multiple antenna outputs, such as a maximum ratio combiner (MRC) and square-law combining (SLC), are used to improve detection reliability. The detection performance of MRC has been analyzed in [22] by using the moment generating function (MGF) of the SNR. Study [25] deduces the exact detection performance analysis by utilizing SLC. Because MRC requires complete knowledge of the channel state information (CSI), a simpler technique is SLC, which does not require the CSI. Moreover, in the processing of the derivation of the detection performance, the MGF approach in [25] provides a more flexible, general framework for analyzing the sensing performance than the PDF approach. This new approach can avoid several difficulties of the PDF method by using a contour integral representation of the Marcum-Q function [26].

In this paper, we first propose an improved MC detector. In the proposed method, we present a reliable simplification for the test statistic of a conventional MC detector. The benefits of the simplification include a reduction in the computational complexity that is caused by computing the test statistic. From analysis, we find that the test statistic of the proposed detector follows a chi-square distribution. The closed-form expressions of the detection probability and false-alarm probability are then derived. Subsequently, SLC is introduced to improve the detection capability, and its contribution is demonstrated by comparing it with the case without SLC. Finally, the sensing performance of the improved MC detector by employing SLC is investigated over Rayleigh, Nakagami-m, and Rician fading channels and composite Rayleigh fading-shadowing channels. The corresponding closed-form average detection probability is derived by using the MGF approach. The effect of fading and shadowing on sensing performance is then demonstrated by simulation

results.

The remainder of this paper is organized as follows. In Section II, we proposed an improved MC detector. In Section III, we derive the closed-form expressions of the detection probability of the proposed detector with SLC in multipath fading and lognormal shadowing environments. Section IV presents numerical and simulation results, and the concluding remarks are provided in Section V.

II. MULTI-CYCLOSTATIONARY (MC) DETECTOR

In this section, we start by analyzing a conventional MC detector. Then, we propose an improved MC detector to reduce the computational complexity by simplifying the test statistic of the conventional detector. Subsequently, the closed-form expressions of the detection probability and false-alarm probability of the proposed detector are derived.

A typical signal detection problem is usually formulated as a binary hypothesis testing problem

$$\begin{cases} H_0 : r(t) = n(t) \\ H_1 : r(t) = h s(t) + n(t) \end{cases} \quad (1)$$

where H_1 denotes the presence of a PU, and H_0 denotes its absence, $r(t)$ is the received signal of the CR user, h is the gain of the channel between the PU and the CR user, $n(t)$ is the additive white Gaussian noise (AWGN), and $s(t)$ is the transmitted signal of the PU. In spectrum sensing, the CR user measures the sufficient statistics at first and then compares them with a threshold that is determined with a desirable false alarm probability in order to decide between two hypotheses.

A. Conventional MC Detector

The sufficient statistic of maximum likelihood (ML) detector is given by [10]

$$Y_{ML} = \int_{t-\frac{T}{2}}^{t+\frac{T}{2}} \int_{t-\frac{T}{2}}^{t+\frac{T}{2}} R_S(u, v) r(u) r^*(v) du dv \quad (2)$$

where $R_S(u, v) = E[s(u)s^*(v)]$ is the autocorrelation function of the transmitted signal $s(t)$, and T is the observation interval. If the signal is cyclostationary, then the ML detector can be expressed as

$$Y_{ML} = \sum_{k=1}^{N_\alpha} \int_{-\infty}^{+\infty} S_s^{\alpha_k}(f)^* S_r^{\alpha_k}(f) df, \alpha_k = \frac{k}{T_c} \quad (3)$$

where $S_s^{\alpha_k}(f)$ and $S_r^{\alpha_k}(f)$ are the spectral correlation functions (SCFs) of $s(t)$ and $r(t)$, respectively, at the k th CF $\alpha_k = k/T_c$, N_α is the number of CFs, $S_s^{\alpha_k}(f)$ is the Fourier transform of the cyclic autocorrelation function $R_r^{\alpha_k}(\tau)$, and the time-independent function $R_r^{\alpha_k}(\tau)$ is calculated as the Fourier-series coefficient of the periodic autocorrelation function $R_r(t, \tau) = \sum_k R_r^{\alpha_k}(\tau) e^{j2\pi\alpha_k t}$ [11], [12]. Because the transmitted signal of the PU is unknown, $S_s^{\alpha_k}(f)$ can be assumed to be a rectangular function with a bandwidth of Δf . Thus,

$$Y_{MC} = \sum_{k=1}^{N_\alpha} \int_{f-\frac{\Delta f}{2}}^{f+\frac{\Delta f}{2}} S_r^{\alpha_k}(v) dv. \quad (4)$$

Consequently, the sum of cyclostationary signal power at all CFs is the sufficient statistic for the optimum detector in ML criterion for cyclostationary signals. This detector is called the MC detector, the total power can be calculated as

$$Y_{MC} = \sum_{k=1}^{N_\alpha} R_r^{\alpha_k}(\tau = 0) \quad (5)$$

where $R_r^{\alpha_k}(\tau = 0)$ represents the cyclostationary signal power at the k th CF.

B. Improved MC Detector

B.1 Simplified test statistic

Because $Y_{MC} = \text{Re}(Y_{MC}) + j\text{Im}(Y_{MC})$ is a complex random variable, the test statistic of a conventional MC detector can be given by [6]

$$T_{MC} = |Y_{MC}|^2 = \sum_{k=1}^{N_\alpha} |R_r^{\alpha_k}(\tau = 0)|^2 + \sum_{k=1}^{N_\alpha} \sum_{n=1, n \neq k}^{N_\alpha} R_r^{\alpha_k}(\tau = 0) R_r^{\alpha_n}(\tau = 0). \quad (6)$$

In order to reduce the computational complexity, we will make a simplification of T_{MC} . Because the second term of T_{MC} brings a large amount of computation, it is omitted here. The first term of T_{MC} is used as the test statistic of the proposed MC detector. Thus, the simplified test statistic of the proposed detector can be defined as

$$T_{\text{sim}} = \sum_{k=1}^{N_\alpha} |R_r^{\alpha_k}(\tau = 0)|^2. \quad (7)$$

B.2 Computational complexity analysis

In order to investigate the computational complexity of T_{MC} and T_{sim} , we perform the following analysis:

- For computing T_{MC} : In (6), we need to perform complex multiplication N_α^2 times and complex addition $(N_\alpha^2 - 1)$ times to compute T_{MC} . Therefore, the total number of T_{MC} is $2N_\alpha^2 - 1$; and thus $\Theta(N_\alpha^2)$ is the computational complexity of the conventional detector.
- For computing T_{sim} : In (7), we need to perform complex multiplication for N_α times and complex addition for $(N_\alpha - 1)$ times to compute T_{sim} ; thus, the total number of computations for T_{sim} is $2N_\alpha - 1$, and $\Theta(N_\alpha)$ is the computational complexity of the proposed detector.

Because $N_\alpha \gg 1$, it can be clearly observed that the computational complexity is greatly reduced by the simplification of the test statistic, which means that the proposed MC detector has lower computational complexity than the conventional detector.

Next, the sensing performance of the proposed detector will be analyzed. By the simulation results in Section IV, we will show that there is no appreciable difference in detection performance between the proposed detector and the conventional detector.

B.3 Sensing performance analysis

Because T_{sim} is the test statistic of the proposed detector, the structure of the detector can be defined as

$$T_{\text{sim}} = \sum_{k=1}^{N_\alpha} |R_r^{\alpha_k}(\tau = 0)|^2 \underset{H_0}{\overset{H_1}{>}} \lambda \quad (8)$$

where λ is the detection threshold.

Consequently, the false-alarm and detection probability of the proposed detector can be represented as

$$P_f = \int_{\lambda}^{+\infty} P(T_{\text{sim}} | H_0) dT_{\text{sim}}, \quad (9)$$

$$P_d = \int_{\lambda}^{+\infty} P(T_{\text{sim}} | H_1) dT_{\text{sim}}. \quad (10)$$

To obtain the conditional probability density functions (pdfs) $P(T_{\text{sim}} | H_0)$ and $P(T_{\text{sim}} | H_1)$, we should focus on $R_r^{\alpha_k}(\tau = 0)$ in (7) first. Let

$$Y_1 = R_r^{\alpha_k}(\tau = 0). \quad (11)$$

The cyclic autocorrelation function of Y_1 can be shown by

$$R_r^{\alpha_k}(\tau) = \lim_{T \rightarrow \infty} \int_{t_0 - \frac{T}{2}}^{t_0 + \frac{T}{2}} r(t + \frac{\tau}{2}) r^*(t - \frac{\tau}{2}) e^{-j2\pi\alpha_k t} dt. \quad (12)$$

From (11) and (12), the discrete-time counterpart of Y_1 is given by

$$Y_1 = \frac{1}{N_S} \sum_{w=1}^{N_S} |r[w]|^2 e^{-j2\pi\alpha_k w}. \quad (13)$$

Hence, H_0 and H_1 according to (1) can be represented as

$$\begin{cases} H_0 : Y_1 = \frac{1}{N_S} \sum_{w=1}^{N_S} |n[w]|^2 e^{-j2\pi\alpha_k w} \\ H_1 : Y_1 = \frac{1}{N_S} \sum_{w=1}^{N_S} |s[w] + n[w]|^2 e^{-j2\pi\alpha_k w} \end{cases} \quad (14)$$

where $n[w] = \text{Re}(n[w]) + j\text{Im}(n[w])$ is a complex AWGN sample with zero mean and variance σ_0^2 , and $s[w]$ is a PU signal sample. The proposed detector can be viewed as computing measures of the signal power for a single cycle frequency α_k , and then the structure of detector can be defined as

$$T_1 = |Y_1|^2 = |R_r^{\alpha_k}(\tau = 0)|^2 \underset{H_0}{\overset{H_1}{>}} \lambda. \quad (15)$$

Therefore, for the case of detection α_k , the detection and false-alarm probability can be represented as

$$P_{f,\alpha_k} = \int_{\lambda}^{\infty} P(T_1 | H_0) dT_1, \quad (16)$$

$$P_{d,\alpha_k} = \int_{\lambda}^{\infty} P(T_1 | H_1) dT_1. \quad (17)$$

Because the pdfs $P(T_1 | H_0)$ and $P(T_1 | H_1)$ can be derived from $P(Y_1 | H_0)$ and $P(Y_1 | H_1)$. Given the central limit theorem for large $N_S, N_\alpha \gg 1$, Y_1 is approximately Gaussian. Since $E\{|n[w]|^2\} = \sigma_0^2$ and $\text{var}\{|n[w]|^2\} = \text{var}\{\text{Re}^2(n[w]) + \text{Im}^2(n[w])\} = \sigma_0^4$, the mean and variance of Y_1 under H_0 are

$$E\{Y_1 | H_0\} = \frac{\sigma_0^2}{N_S} \sum_{w=1}^{N_S} e^{-j2\pi\alpha_k w} = 0, \quad (18)$$

$$\text{var}\{Y_1 | H_0\} = \frac{1}{N_S} \sum_{w=1}^{N_S} |e^{-j2\pi\alpha_k w}|^2 \text{var}\{|n[w]|^2\} = \frac{\sigma_0^4}{N_S}. \quad (19)$$

Because $\{Y_1 | H_0\} = \text{Re}(Y_1 | H_0) + j\text{Im}(Y_1 | H_0)$ is a complex Gaussian random variable, then $(T_1 | H_0) = \{Y_1 | H_0\}^2 = [\text{Re}(Y_1 | H_0)]^2 + [\text{Im}(Y_1 | H_0)]^2$ follows a central χ^2 distribution with two degrees of freedom, which has following probability density function

$$P(T_1 | H_0) = \frac{1}{2\sigma_1^2} e^{-\frac{T_1}{2\sigma_1^2}}, \quad \sigma_1^2 = \frac{\sigma_0^4}{N_S}. \quad (20)$$

Thus, the false alarm probability for detection α_k is

$$P_{f,\alpha_k} = e^{-\frac{\lambda}{2\sigma_1^2}}. \quad (21)$$

Similarly, because $E\{|s[w] + n[w]|^2\} = |s[w]|^2 + \sigma_0^2$, the mean of $(Y_1 | H_1)$ is

$$\begin{aligned} E\{Y_1 | H_1\} &= \frac{1}{N_S} \sum_{w=1}^{N_S} (|s[w]|^2 + \sigma_0^2) e^{-j2\pi\alpha_k w} \\ &= \frac{1}{N_S} \sum_{w=1}^{N_S} |s[w]|^2 e^{-j2\pi\alpha_k w} = P_{\alpha_k} \end{aligned} \quad (22)$$

where complex-valued P_{α_k} is the signal power at the k th CF α_k . Because noise samples are statistically independent, the variance of $(Y_1 | H_1)$ is

$$\begin{aligned} \text{var}\{Y_1 | H_1\} &= \frac{1}{N_S^2} \sum_{w=1}^{N_S} |e^{-j2\pi\alpha_k w}|^2 \text{var}\{|s[w]|^2 + |n[w]|^2\} \\ &= \frac{2\sigma_0^2 P}{N_S} + \frac{\sigma_0^4}{N_S} \end{aligned} \quad (23)$$

where $P = \frac{1}{N_S} \sum_{w=1}^{N_S} |s[w]|^2$. Therefore, $(T_1 | H_1) = \{Y_1 | H_1\}^2 = [\text{Re}(Y_1 | H_1)]^2 + [\text{Im}(Y_1 | H_1)]^2$ is non-central χ^2 distribution with two degrees of freedom, and its pdf is given by

$$P(T_1 | H_1) = \frac{1}{2\sigma_2^2} e^{-\frac{T_1 + u_1}{2\sigma_2^2}} I_0\left(\frac{\sqrt{T_1} u_1}{\sigma_2^2}\right) \quad (24)$$

where $u_1 = \sqrt{\{E[\text{Re}(Y_1 | H_1)]\}^2 + \{E[\text{Im}(Y_1 | H_1)]\}^2} = |P_{\alpha_k}|$ and $\sigma_2^2 = 2\sigma_0^2 P / N_S + \sigma_0^4 / N_S$. The corresponding detection probability can then be given by

$$P_{d,\alpha_k} = Q_1\left(\frac{u_1}{\sigma_2}, \frac{\sqrt{\lambda}}{\sigma_2}\right) \quad (25)$$

where $Q_1(\cdot, \cdot)$ is the generalized Marcum-Q function.

The above derivation shows that the detection and false-alarm probability of proposed detector when it measures a single CF α_k . However, the test statistic $T_{\text{sim}} = \sum_{k=1}^{N_\alpha} |R_r^{\alpha_k}(\tau=0)|^2 = \sum_{k=1}^{N_\alpha} T_1$, which means there are N_α different CFs should be measured by proposed detector. Because T_1 follows a central χ^2 distribution with two degrees of freedom under H_0 and a non-central χ^2 distribution with two degrees of freedom under H_1 , it can be easily concluded that T_{sim} follows a central χ^2 distribution with $2N_\alpha$ degrees of freedom under H_0 and a non-central χ^2 distribution with $2N_\alpha$ degrees of freedom under H_1 . The conditional pdfs of T_{sim} can then be represented as

$$P(T_{\text{sim}} | H_0) = \frac{1}{2^{N_\alpha} \sigma_1^{2N_\alpha} \Gamma(N_\alpha)} e^{-\frac{T_{\text{sim}}}{2\sigma_1^2}} T_{\text{sim}}^{N_\alpha-1}, \quad \sigma_1^2 = \frac{\sigma_0^4}{N_S}, \quad (26)$$

$$\begin{aligned} P(T_{\text{sim}} | H_1) &= \frac{1}{2\sigma_2^2} e^{-\frac{T_{\text{sim}} + u_2}{2\sigma_2^2}} \left(\frac{T_{\text{sim}}}{u_2}\right)^{\frac{N_\alpha-1}{2}} \frac{1}{\Gamma(N_\alpha-1)} \left(\frac{\sqrt{T_{\text{sim}} u_2}}{\sigma_2^2}\right), \\ \sigma_2^2 &= \frac{2\sigma_0^2 P}{N_S} + \frac{\sigma_0^4}{N_S} \end{aligned} \quad (27)$$

where $u_2 = \sum_{k=1}^{N_\alpha} u_1 = \sum_{k=1}^{N_\alpha} |P_{\alpha_k}|$, $I_\nu(\cdot)$ is the ν -th-order modified Bessel function of the first kind and $\Gamma(\cdot)$ is the gamma function. The corresponding false alarm and detection probabilities of proposed detector are

$$P_f = \int_{\lambda}^{+\infty} P(T_{\text{sim}} | H_0) dT_{\text{sim}} = \frac{\Gamma\left(N_\alpha, \frac{\lambda}{2\sigma_1^2}\right)}{\Gamma(N_\alpha)}, \quad (28)$$

$$P_d = \int_{\lambda}^{+\infty} P(T_{\text{sim}} | H_1) dT_{\text{sim}} = Q_{N_\alpha}\left(\frac{\sqrt{u_2}}{\sigma_2}, \frac{\sqrt{\lambda}}{\sigma_2}\right). \quad (29)$$

Because the proposed detector is in an AWGN channel (i.e., $h_i = 1$), $u_2 = \sum_{k=1}^{N_\alpha} |P_{\alpha_k}|$ is the signal power, σ_0^2 is noise power, and γ denote the SNR, then $\gamma = u_2 / \sigma_0^2$. Thus, (29) can be rewritten as

$$P_d = Q_{N_\alpha}\left(\frac{\sigma_0 \sqrt{\gamma}}{\sigma_2}, \frac{\sqrt{\lambda}}{\sigma_2}\right). \quad (30)$$

III. SENSING PERFORMANCE OF PROPOSED DETECTOR WITH MULTIPLE ANTENNAS IN MULTIPATH FADING AND LOGNORMAL SHADOWING ENVIRONMENTS

As shown in Fig. 1, we consider a CR user with L antennas and assume that the PU has a single antenna. SLC is employed

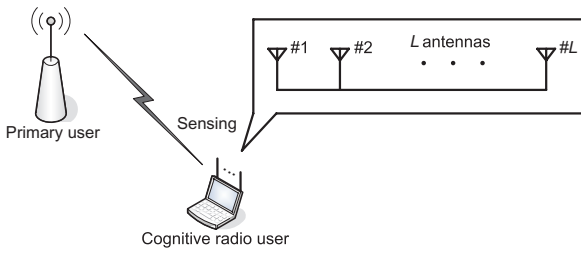


Fig. 1. Spectrum sensing with L antennas.

to combine the outputs of L antennas. We also assume a narrowband wireless system [30].

In this section, we first derive the detection probability and false alarm probability of the proposed MC detector with SLC diversity over an AWGN channel. Then, fading channels such as Rayleigh, Nakagami- m , and Rician are considered. Finally, the sensing performance over a Rayleigh fading and lognormal shadowing channel is investigated.

A. Square-Law Combining (SLC)

In SLC scheme, the outputs of the square-law devices (square-and-integrate operation per antenna) are added to yield a new test statistic T_{sim_Σ} . Therefore, the new test statistic T_{sim_Σ} can be written by

$$T_{\text{sim}_\Sigma} = \sum_{i=1}^L T_{\text{sim}_i} \quad (31)$$

where T_{sim_i} denotes the test statistic from the i th square-law device.

Note that the decision is made in a local user if SLC technologies are employed in the local cognitive user. On the other hand, the decision is carried out in a fusion center when SLC is used in a cognitive radio network, i.e., cooperative sensing.

B. SLC over AWGN Channel

If SLC is employed to improve the sensing performance of the proposed detector over an AGWN channel, the test statistic T_{sim_Σ} follows a centrality chi-square distribution with LN_α degrees of freedom under H_0 . Therefore, the false alarm probability becomes

$$P_{f,\text{SLC}} = P(T_{\text{sim}_\Sigma} > \lambda | H_0) = \frac{\Gamma(LN_\alpha, \frac{\lambda}{2\sigma_1^2})}{\Gamma(LN_\alpha)}. \quad (32)$$

Similarly, under H_1 , T_{sim_Σ} has a non-central chi-square distribution with LN_α degrees of freedom, and a non-centrality parameter $2\gamma_t = 2 \sum_{i=1}^L \gamma_i$. Thus, the detection probability can be obtained as

$$P_{d,\text{SLC}} = P(T_{\text{sim}_\Sigma} > \lambda | H_1) = Q_{LN_\alpha} \left(\frac{\sigma_0 \sqrt{\gamma_t}}{\sigma_2}, \frac{\sqrt{\lambda}}{\sigma_2} \right). \quad (33)$$

C. SLC in Multipath Fading and Lognormal Shadowing Environments

In fading and shadowing environments, P_f of (32) will remain constnt since P_f is considered for the case of no signal transmission and as such is independent of SNR. Therefore, we will derive the average detection probability ($\overline{P_d}$) by using MGF over Rayleigh, Nakagami- m , Rician, and composite Rayleigh fading-shadowing channels, respectively.

C.1 Average detection probability - MGF approach

The generalized Marcum-Q function in (33) can be written as a circular contour integral within the contour radius $r \in [0, 1)$. Then, the (33) can be represented as

$$P_{d,\text{SLC}} = \frac{e^{-\frac{\lambda}{2\sigma_2^2}}}{2\pi j} \oint_{\Delta} \frac{e^{-\frac{\sigma_0^2}{2\sigma_2^2}(\frac{1}{z}-1)\gamma_t + \frac{\lambda}{2\sigma_2^2}z}}{z^{LN_\alpha}(1-z)} dz \quad (34)$$

where Δ is a circular contour of radius $r \in [0, 1)$.

The MGF of the average received SNR $\overline{\gamma}_t$ is $M_{\overline{\gamma}_t}(s) = E(e^{-s\overline{\gamma}_t})$, where $E(\cdot)$ is the expectation. Thus, the average detection probability, $\overline{P}_{d,\text{SLC}}$, is given by

$$\overline{P}_{d,\text{SLC}} = \frac{e^{-\frac{\lambda}{2\sigma_2^2}}}{2\pi j} \oint_{\Delta} f(z) dz \quad (35)$$

where $f(z) = M_{\overline{\gamma}_t} \left(\frac{\sigma_0^2}{2\sigma_2^2} \left(1 - \frac{1}{z}\right) \right) e^{\frac{\lambda}{2\sigma_2^2}z} / z^{LN_\alpha}(1-z)$.

In our study, the expression in (35) is fairly general and holds for any case where the MGF is available in a suitable form.

C.2 Average detection probability over Rayleigh fading channel

The MGF of Rayleigh fading combined with SLC is

$$M_{\overline{\gamma}_t,\text{SLC}}^{\text{Ray}}(s) = (1 + \overline{\gamma}_t s)^{-L}. \quad (36)$$

After substituting this MGF in (35), the average detection probability, $\overline{P}_{d,\text{SLC}}$, over Rayleigh channel can be written in the

form of (35) with $f(z) = \frac{e^{\frac{\lambda}{2\sigma_2^2}z}}{(1+\mu_1)^L (z-\theta_1)^L z^{\beta_1}(1-z)}$, where $\mu_1 = \sigma_0^2 \overline{\gamma}_t / 2\sigma_2^2$, $\theta_1 = \mu_1 / (1 + \mu_1)$ and $\beta_1 = L(N_\alpha - 1)$.

In radius $r \in [0, 1)$, there are β_1 poles at the origin $z = 0$ and L pole at $z = \theta_1$. By applying the residue theorem to (35), the detection probability over Rayleigh fading is obtained as (37).

The residue $\text{Res}(f; 0, \beta_1)$ and residue $\text{Res}(f; \theta_1, L)$ of (37) are given by

$$\text{Res}(f; 0, \beta_1) = \frac{D^{\beta_1-1} \left(\frac{e^{\frac{\lambda}{2\sigma_2^2}z}}{(1-z)(z-\theta_1)^L} \right) \Big|_{z=0}}{(1+\mu_1)^L (\beta_1 - 1)!}, \quad (39)$$

$$\text{Res}(f; \theta_1, L) = \frac{D^{L-1} \left(\frac{e^{\frac{\lambda}{2\sigma_2^2}z}}{(1-z)z^{\beta_1}} \right) \Big|_{z=\theta_1}}{(1+\mu_1)^L (L - 1)!} \quad (40)$$

where $D^n(f(z))$ denotes the n th derivative of $f(z)$ with respect to z .

$$\overline{P_{d,SLC}^{\text{Ray}}} = \begin{cases} e^{-\frac{\lambda}{2\sigma_2^2}} [\text{Res}(f; 0, \beta_1) + \text{Res}(f; \theta_1, L)] & N_\alpha > L \\ e^{-\frac{\lambda}{2\sigma_2^2}} \text{Res}(f; \theta_1, L) & N_\alpha \leq L \end{cases} \quad (37)$$

$$\overline{P_{d,SLC}^{\text{Nak}}} = \begin{cases} e^{-\frac{\lambda}{2\sigma_2^2}} [\text{Res}(f; 0, \beta_2) + \text{Res}(f; \theta_2, Lm)] & N_\alpha > Lm \\ e^{-\frac{\lambda}{2\sigma_2^2}} \text{Res}(f; \theta_2, Lm) & N_\alpha \leq Lm \end{cases} \quad (38)$$

C.3 Average detection probability over Nakagami- m fading channel

The MGF of Nakagami- m fading combined with SLC is

$$M_{\overline{\gamma}_t, \text{Nak}}(s) = (1 + \overline{\gamma}_t s)^{-Lm}. \quad (41)$$

The detection probability over Nakagami- m channel can be written in the form of (35) with $f(z) = e^{\lambda/2\sigma_2^2 z} / (1 + \mu_2)^{Lm} (z - \theta_2)^{Lm} z^{\beta_2} (1 - z)$, where $\mu_2 = \sigma_0^2 \overline{\gamma}_t / 2\sigma_2^2 m$, $\theta_2 = \mu_2 / (1 + \mu_2)$ and $\beta_2 = L(N_\alpha - m)$. Following a similar procedure as in the Rayleigh fading case, the detection probability over a Nakagami- m channel can be obtained as follows:

The residue $\text{Res}(f; 0, \beta_2)$ and residue $\text{Res}(f; \theta_2, Lm)$ of (38) are given by

$$\text{Res}(f; 0, \beta_2) = \frac{D^{\beta_2-1} \left(\frac{e^{\frac{\lambda}{2\sigma_2^2} z}}{(1-z)(z-\theta_2)^{Lm}} \right) \Big|_{z=0}}{(1 + \mu_2)^{Lm} (\beta_2 - 1)!}, \quad (42)$$

$$\text{Res}(f; \theta_2, Lm) = \frac{D^{Lm-1} \left(\frac{e^{\frac{\lambda}{2\sigma_2^2} z}}{(1-z)z^{\beta_2}} \right) \Big|_{z=\theta_2}}{(1 + \mu_2)^{Lm} (Lm - 1)!}. \quad (43)$$

From the above analysis, we notice that the results are limited to an integer Lm and allow us to compute $\overline{P_{d,SLC}^{\text{Nak}}}$ for certain non-integer values of m . For example, $\overline{P_{d,SLC}^{\text{Nak}}}$ over a two branch case can be computed for $1/2$ multiples of m values. We also notice that a Rayleigh fading channel is a special case of a Nakagami- m channel, for which $\overline{P_{d,SLC}^{\text{Ray}}}$ can be obtained by substituting $m = 1$ in (38).

C.4 Average detection probability over Rician fading channel

The MGF of Rician fading combined with SLC is given by

$$M_{\overline{\gamma}_t, \text{SLC}}^{\text{Ric}}(s) = \left(\frac{1 + K}{1 + K + s\overline{\gamma}_t} \right)^L \exp \left(-\frac{LKs\overline{\gamma}_t}{1 + K + s\overline{\gamma}_t} \right) \quad (44)$$

where K is the Rice factor. Notice that for the special case of $K = 0$ (Rayleigh fading), (44) reduces to Rayleigh in (36). Hence, using (44), the average detection probability over Rician fading is obtained as

$$\overline{P_{d,SLC}^{\text{Ric}}} = \frac{A}{2\pi j} \oint_{\Delta} \frac{e^{\frac{a}{z-\theta_3}}}{(z-\theta_3)} f(z) dz \quad (45)$$

where $f(z) = \frac{e^{\frac{\lambda}{2\sigma_2^2} z}}{(1+K+\mu_2)^L (z-\theta_3)^{L-1} z^{\beta_2} (1-z)}$, $\theta_3 = \frac{\mu_2}{\mu_2 + K + 1}$, $A = e^{-\frac{\lambda}{2\sigma_2^2}} [(1+K)e^{-K\theta_3}]^L$, and $a = LK\theta_3(1-\theta_3)$.

Applying a Laurent series expansion for $\frac{e^{\frac{a}{z-\theta_3}}}{(z-\theta_3)}$ in (45) when $K \neq 0$ and using the residue theorem to integrate term by term, the average detection probability over Rician fading can be derived as (46).

The residue $\text{Res}(f; 0, \beta_2)$ and residue $\text{Res}(f; \theta_3, L+n-1)$ of (46) are given by

$$\text{Res}(f; 0, \beta_2) = \frac{D^{\beta_2-1} \left(\frac{e^{\frac{\lambda}{2\sigma_2^2} z}}{(1-z)(z-\theta_3)^{L+n-1}} \right) \Big|_{z=0}}{(1 + K + \mu_2)^L (\beta_2 - 1)!}, \quad (48)$$

$$\text{Res}(f; \theta_3, L+n-1) = \frac{D^{L+n-2} \left(\frac{e^{\frac{\lambda}{2\sigma_2^2} z}}{(1-z)z^{\beta_2}} \right) \Big|_{z=\theta_3}}{(1 + K + \mu_2)^L (L+n-2)!}. \quad (49)$$

C.5 Average detection probability over Rayleigh fading and lognormal shadowing channel

Because a shadowing process is typically modeled as lognormal distribution, the Rayleigh fading-lognormal shadowing channel model follows a gamma-lognormal distribution as [17]

$$g_{\gamma N}(x) = \sum_{i=1}^N \phi_i e^{-\varepsilon_i x}, \quad x \geq 0, \phi_i \geq 0, \varepsilon_i \geq 0 \quad (50)$$

where $\phi_i = \rho_i e^{-(\sqrt{2}\delta\eta_i + \psi)} / (\sqrt{\pi} \sum_{i=1}^N \rho_i)$, N is the number of terms in the mixture, $\varepsilon_i = e^{-(\sqrt{2}\delta\eta_i + \psi)}$, η_i and ρ_i are the abscissas and weight factors for the Gaussian-Laguerre integration, respectively, and ψ and δ are the mean and the standard deviation of the lognormal distribution, respectively. The MGF of Rayleigh fading-lognormal shadowing combined with SLC is given by

$$M_{\gamma N}(s) = \sum_{i=1}^N \left(\frac{\phi_i}{\varepsilon_i + s} \right)^L. \quad (51)$$

$$\overline{P_{d,SLC}^{Ric}} = \begin{cases} A \sum_{n=1}^{a^{n-1}} [\text{Res}(f; 0, \beta_2) + \text{Res}(f; \theta_3, L + n - 1)] & N_\alpha > L + n - 1 \\ A \sum_{n=1}^{a^{n-1}} \text{Res}(f; \theta_3, L + n - 1) & N_\alpha \leq L + n - 1 \end{cases} \quad (46)$$

$$\overline{P_{d,SLC}^{R1}} = \begin{cases} e^{-\frac{\lambda}{2\sigma_2^2}} \sum_{i=1}^N \left(\frac{\phi_i}{\varepsilon_i}\right)^L [\text{Res}(f_i; 0, \beta_1) + \text{Res}(f_i; \theta_i, L)] & N_\alpha > L \\ e^{-\frac{\lambda}{2\sigma_2^2}} \sum_{i=1}^N \left(\frac{\phi_i}{\varepsilon_i}\right)^L \text{Res}(f_i; \theta_i, L) & N_\alpha \leq L \end{cases} \quad (47)$$

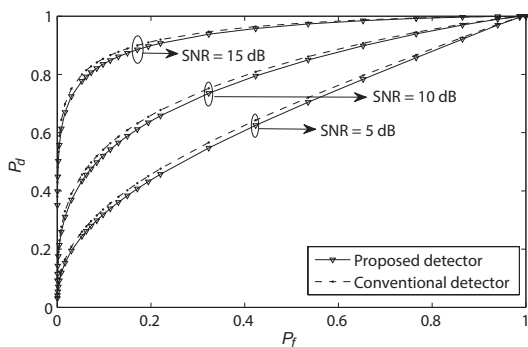


Fig. 2. ROC curves for the proposed and conventional MC detector with different SNRs over AWGN channel ($\gamma = \{5, 10, \text{and } 15 \text{ dB}\}$, $N_\alpha = 10$).

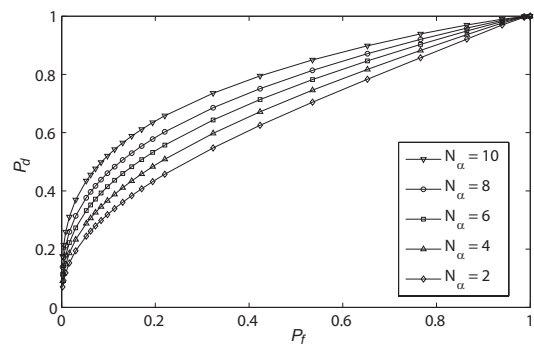


Fig. 3. ROC curves for the proposed detector over AWGN channel with different N_α s ($N_\alpha = 2, 4, 6, 8, \text{and } 10$, $\gamma = 10 \text{ dB}$).

Thus, the average detection probability over Rayleigh fading-lognormal shadowing channel, $\overline{P_{d,SLC}^{R1}}$, can be evaluated in closed-form as (47), where $f_i(z) = \frac{e^{-\frac{\lambda}{2\sigma_2^2}z}}{(1+\mu_i)^L \left(z - \frac{\mu_i}{1+\mu_i}\right)^L z^{\beta_1}(1-z)}$, $\mu_i = \sigma_0^2/2\sigma_2^2\varepsilon_i$ and $\theta_i = \mu_i/(1+\mu_i)$. Following a similar procedure as in the Rayleigh fading case, the residues $\text{Res}(f_i; 0, \beta_1)$ and $\text{Res}(f_i; \theta_i, L)$ can be obtained; however, we omit the expressions here for brevity.

IV. NUMERICAL RESULTS AND ANALYSIS

In this section, we provide analytical and simulation results to verify the analytical framework. In order to show the sensing performance of the proposed detector, we plot the receiver operating characteristic (ROC) curves (plots of detection probability P_d vs. false alarm probability P_f) and complementary ROC curves (plots of miss detection probability P_m versus false alarm probability P_f), P_d vs. average SNR curves and P_d vs. L curves. Note that each of the following figures contains both analytical result and simulation result, which are represented by lines and discrete marks, respectively.

To verify the reliability and efficiency of the proposed detector, we perform the following analysis: (1) Reliability analysis:

Fig. 2 shows the ROC curves of the proposed MC detector and conventional MC detector over an AWGN channel, for different SNR $\gamma = 5, 10, \text{and } 15 \text{ dB}$ and $N_\alpha = 10$. It can be observed that the analytical results match well with the results from the simulation, confirming the accuracy of the analysis. In Fig. 2, there is a slight difference in sensing performance between the proposed and conventional detector because of the simplification of the test statistic of the conventional detector. Although the simplification slightly degrades sensing accuracy, a satisfactory sensing capability is still maintained. (2) Computational complexity analysis: Based on the analysis in Section II-B-2, the computational complexity of the conventional MC detector is $\Theta(10^2)$, whereas that for the proposed detector is $\Theta(10)$ for $N_\alpha = 10$. The analysis above clearly illustrated that the proposed detector is more efficient than the conventional detector. Overall, Fig. 2 and the computational complexity analysis verify that the proposed MC detector can reduce the computational complexity while still maintaining sufficient detection sensitivity.

To further investigate the sensing performance of the proposed detector, we plot the ROC curves with different values of N_α , for $N_\alpha = 2, 4, 6, 8, \text{and } 10$. In Fig. 3, the sensing performance improves with an increasing value of N_α , the sensing performance improves, which is similar to conventional detector. which is similar to the performance of a conventional detector.

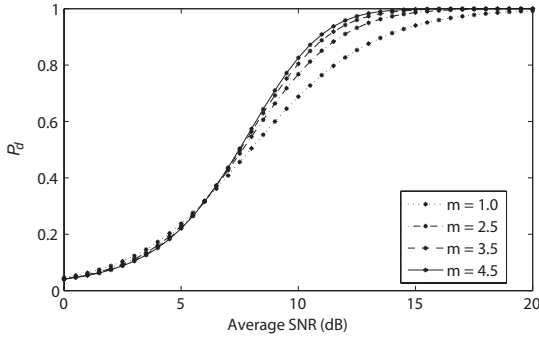


Fig. 4. P_d vs. average SNR curves for the proposed detector over Rayleigh and Nakagami- m fading channels ($m = 1.0, 2.5, 3.5, 4.5, L = 2, P_d = 0.01, N_\alpha = 10$).

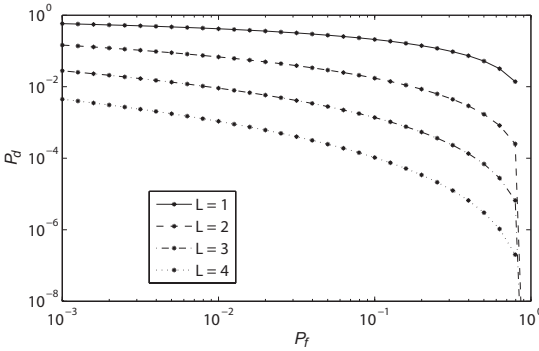


Fig. 5. Complementary ROC curves with SLC over Rician fading channel ($\overline{\gamma_t} = 10$ dB, $L = \{1, 2, 3, 4\}, K = 4, N_\alpha = 10$).

tor. Because the MC detector measures the sum of N_α spectral correlation function, the higher N_α is, the more accurate binary decision the detector makes.

Fig. 4 depicts depicts the P_d vs. average SNR curves of the proposed detector over Rayleigh and Nakagami- m fading channels, for Nakagami parameter $m = 1, 2.5, 3.5, 4.5, L = 2, P_d = 0.01, N_\alpha = 10$. Here, we consider both the integer and non-integer values of Nakagami parameter m . Rayleigh curve coincide with the Nakagami $m = 1$ curve and therefore not shown. For Nakagami- m fading, it can be observed that the higher m is, the better the detector works. Moreover, the difference on sensing performance between the case where $m = 1.0$ and the case where $m = 2.5$ is remarkable, while the difference is smaller with further increase of m . That is to say, greater values of the fading index m and higher values of the average SNR imply a relatively less degraded received signal and thus lead to a higher detection probability.

Fig. 5 shows the complementary ROC curves of the proposed detector over a Rician fading channel with SLC, for $K = 4$ and $\overline{\gamma_t} = 10$ dB. The number of diversity branches varies from one to four. It can be observed that the sensing capability of single branch ($L = 1$, non-SLC) case is the lowest bound of the sensing ability of the proposed detector. There is a significant improvement in the sensing capability of the proposed detector with an increasing number of SLC branches.

Fig. 6 depicts the ROC curves of the proposed detector over a Rayleigh fading and lognormal shadowing channel without

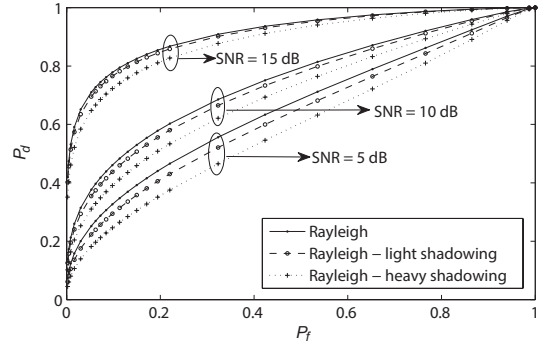


Fig. 6. ROC curves of proposed detector without SLC over Rayleigh and Rayleigh fading and lognormal shadowing channels ($N_\alpha = 10$).

SLC. The shadowing effects considered here were introduced by Loo in [18] and are (i) light shadowing ($\psi = 0.115$ and $\delta = 0.115$), which corresponds to sparse tree cover and (ii) heavy shadowing ($\psi = 3.914$ and $\delta = 0.806$), which corresponds to dense tree cover. We take $N = 10$ in (50), which makes the mean square error (MSE) between the exact gamma-lognormal channel model and the approximated mixture gamma channel model in (44) less than 10^{-4} . The numerical results match well with the results from the theoretical analysis, confirming the accuracy of the analysis. It can be observed that the performance of the proposed detector degrades with increase in Rayleigh fading and lognormal shadowing environments, and improves at higher SNR. Further, for Rayleigh and Rayleigh fading and *light* shadowing environments, there is a slight difference in the detector’s performance. However, there is a significant performance degradation in the proposed detector because of the *heavy* shadowing effect in lower average SNR (e.g., 5 dB).

Next, we consider the effect of SLC in alleviating the Rayleigh fading and lognormal shadowing. Fig. 7 demonstrate that SLC improves the detection performance, even in serious Rayleigh fading and lognormal shadowing environments. For example, in a Rayleigh and *heavy* shadowing environment with a low average SNR (e.g., 5 dB), we find that the detection probability for the four branch SLC case ($L = 4$) is almost six times that for a single branch non-SLC case ($L = 1$). Furthermore, for the two branch SLC case ($L = 2$), there is approximately 3 dB performance gain compared with the non-SLC case. Therefore, the SLC mitigates the impact of fading and lognormal shadowing and introduces a significant improvement in the detection probability.

V. CONCLUSION

In this paper, the sensing performance of an improved MC detector with multiple antennas in fading and shadowing environments has been studied. We first proposed an improved MC detector. By simplifying the test statistic of the conventional MC detector, the computational complexity is reduced while maintaining sufficient accuracy in the sensing performance. The closed-form expressions of the detection probability and false alarm probability were derived. Subsequently, the sensing per-

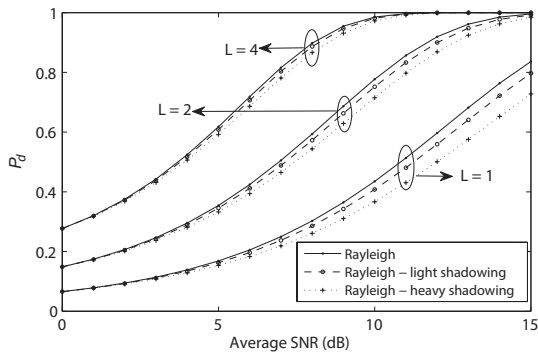


Fig. 7. P_d vs. average SNR with SLC over Rayleigh and Rayleigh fading and lognormal shadowing channels ($P_f = 0.01$, $L = \{1, 2, 4\}$, $N_\alpha = 10$).

formance of the proposed detector by employing SLC was investigated in fading and shadowing environments. For Rayleigh, Nakagami- m , and Rician fading and Rayleigh fading and lognormal shadowing channels, the closed-form expressions of the detection probability were derived by using the MGF approach, respectively. Illustrative and analytical results show that although multipath fading and lognormal shadowing degrade the sensing performance of the proposed detector, the gain is significantly improved by SLC. Although a Rayleigh fading and lognormal shadowing channel is analyzed here, the analytical framework can be extended to a Nakagami fading and lognormal shadowing channel in future work, which is considered as a generic fading-shadowing channel model. These results will help quantify the performance gains for an MC detector with multiple antennas in fading and shadowing environments, which can help emerging applications such as cognitive radio and ultra-wideband radio.

ACKNOWLEDGMENTS

This work is supported by the National Natural Science Foundation of China (61227801, 61121001), the National Key Technology Research and Development Program of China (2012ZX03003006, 2012ZX03006003-003, 2013ZX03003014-003), the National Science and Technology Major Project (2011ZX03004-003), the Program for New Century Excellent Talents in University (NCET-01-0259), the National college students innovation experiment program of China (ZCC016236) and the Fundamental Research Funds for the Central Universities (2013RC0106).

REFERENCES

- [1] J. Mitola, "Cognitive radio: An integrated agent architecture for software defined radio," Ph.D. dissertation, *KTH Royal Institute of Technology*, Sweden, May 2000.
- [2] K. Sridhara, A. Chandra, and P. S. M. Tripathi, "Spectrum challenges and solutions by cognitive radio: An overview," *Wireless Pers. Commun.*, vol. 45, no. 3, pp. 281–291, 2008.
- [3] W. El-Hajj, H. Safa, and M. Guizani, "Survey of security issues in cognitive radio networks," *J. Internet Technol.*, vol. 12, no. 2, pp. 181–198, 2011.
- [4] Y. Chen, C. Cho, I. You, and H. Chao, "A cross-layer protocol of spectrum mobility and handover in cognitive LTE networks," *Simul. Model. Pract. Theory*, vol. 19, no. 8, pp. 1723–1744, 2011.
- [5] H. Arslan, "Cognitive radio, software defined radio, and adaptive wireless systems," *Springer*, 2007.
- [6] L. Huang, Z. Gao, D. Guo, H. Chao, and J. Park, "A sensing policy based on the statistical property of licensed channel in cognitive network," *Int. J. Internet Protocol Technol.*, vol. 5, no. 4, pp. 219–229, 2010.
- [7] Z. Gao, L. Huang, Y. Yao, and T. Wu, "Performance analysis of a busycognitive multi-channel MAC protocol," *J. Internet Technol.*, vol. 11, no. 3, pp. 299–306, 2011.
- [8] S. Haykin, "Cognitive radio: Brain-empowered wireless communications," *IEEE J. Sel. Areas Commun.*, vol. 23, no. 2, pp. 201–220, Feb. 2005.
- [9] A. Ghasemi and E. S. Sousa, "Spectrum sensing in cognitive radio networks: The cooperation-processing tradeoff," *Wireless Commun. Mobile Comput.*, vol. 7, no. 9, pp. 1049–1060, Nov. 2007.
- [10] S. M. Mishra, A. Sahai, and R. W. Brodersen, "Cooperative sensing among cognitive radios," *Int. Conf. Communications*, Istanbul, Turkey, June 2006.
- [11] A. V. Dandawate and G. B. Giannakis, "Statistical tests for presence of cyclostationarity," *IEEE Trans. Signal Process.*, vol. 42, no. 9, pp. 2355–2369, Sept. 1994.
- [12] W. A. Gardner, "Signal interception: A unifying theoretical framework for feature detection," *IEEE Trans. Commun.*, vol. 36, pp. 897–906, 1988.
- [13] J. Wang, T. Chen, and B. Huang, "Cyclo-period estimation for discrete time cyclo-stationary signals," *IEEE Trans. Signal Process.*, vol. 54, no. 1, pp. 83–94, 2006.
- [14] R. Tandra and A. Sahai, "Fundamental limits on detection in low SNR under noise uncertainty," in *Proc. Wireless Commun. Symp. on Signal Processing*, 2005.
- [15] M. Derakhshani, M. Nasiri-Kenari, and T. Le-Ngoc, "Cooperative cyclostationary spectrum sensing in cognitive radios at low SNR regimes," *IEEE Trans. Wireless Commun.*, vol. 10, no. 11, pp. 3754–3764, 2012.
- [16] A. Pandharipande and J. P. Linnartz, "Performance analysis of primary user detection in multiple antenna cognitive radio," in *Proc. of IEEE International Conf. on Commun.*, *IEEE Press*, 2007, pp. 6482–6486.
- [17] S. Atapattu, C. Tellambura, and H. Jiang, "Energy detection based cooperative spectrum sensing in cognitive radio networks," *IEEE Trans. Wireless Commun.*, vol. 10, no. 4, pp. 1232–1242, 2011.
- [18] C. Loo, "Digital Transmission through a land mobile satellite channel," *IEEE Trans. Wireless Commun.*, vol. 38, pp. 693–697, 1990.
- [19] S. P. Herath, N. Rajatheva, and C. Tellambura, "Energy detection of unknown signals in fading and diversity reception," *IEEE Trans. Wireless Commun.*, vol. 59, no. 9, pp. 2443–2453, 2011.
- [20] Z. Quan, S. Cui, and A. H. Sayed, "Feature detection based on multiple cyclic frequencies in cognitive radios," in *Proc. IEEE Microwave Conf.*, Sept. 2008.
- [21] K. W. Choi, W. S. Jeon, and D. G. Jeong, "Sequential detection of cyclostationary signal for cognitive radio systems," *IEEE Trans. Wireless Commun.*, vol. 8, no. 9, pp. 4480–4485, Sept. 2009.
- [22] K. L. Du and W. H. Mow, "Affordable cyclostationarity-based spectrum sensing for cognitive radio with smart antennas," *IEEE Trans. Veh. Technol.*, vol. 59, no. 4, pp. 1877–1886, May 2010.
- [23] J. Lunden, V. Koivunen, A. Huttunen, and H. V. Poor, "Collaborative cyclostationary spectrum sensing for cognitive radio systems," *IEEE Trans. Signal Process.*, vol. 57, no. 11, pp. 4182–4195, Nov. 2009.
- [24] H. Sadeghi and P. Azmi, "Cyclostationarity-based cooperative spectrum sensing for cognitive radio networks," in *Proc. IEEE IST*, Aug. 2008.
- [25] M. Derakhshani, M. Nasiri-Kenari, and T. Le-Ngoc, "Cooperative cyclostationary spectrum sensing in cognitive radios at low SNR regimes," *IEEE Trans. Wireless Commun.*, vol. 10, no. 11, pp. 3754–3764, 2012.
- [26] C. Tellambura, A. Annamalai, and V. K. Bhargava, "Closed form and infinite series solutions for the MGF of a dual-diversity selection combiner output in bivariate Nakagami- m fading," *IEEE Trans. Wireless Commun.*, vol. 51, no. 4, pp. 539–542, 2003.
- [27] H. L. Van Trees, *Detection, Estimation, and Modulation Theory, Part III*, Wiley, 2001.
- [28] W. A. Gardner, *Cyclostationarity in Communications and Signal Processing*, *IEEE Press*, 1994.
- [29] W. A. Gardner and M. S. Spooner, "Signal interception: Performance advantages of cyclic-feature detectors," *IEEE Trans. Wireless Commun.*, vol. 40, no. 1, pp. 149–159, 1992.
- [30] A. Goldsmith, *Wireless Communications*, *Cambridge University Press*, 2005.



Ying Zhu is currently a Ph.D. candidate at Beijing University of Posts and Telecommunications (BUPT), Beijing, China. Her research interests include spectrum sensing, resource sharing, and resource management in cognitive radio networks.



Zhiyong Feng received her M.S. and Ph.D. degrees from BUPT, China. She is a professor at BUPT and is currently leading the Ubiquitous Network Lab in the Wireless Technology Innovation (WTI) Institute. She is a member of IEEE and active in standards development, including ITU-R WP5A/WP5D, IEEE 1900, ETSI, and CCSA. Her main research interests include cognitive wireless networks, convergence of heterogeneous wireless networks, spectrum sensing, dynamic spectrum management, and cross-layer design.



Jia Liu received an M.S. degree in Electronics and Information Engineering from Guilin University of Electronic Technology, Guilin, China, in 2008. He is currently working toward a Ph.D. degree in communication and information systems at the School of Electronic Engineering, Beijing University of Posts and Telecommunications, Beijing, China. His research interests include cognitive radio, relay, and wireless network coding.



Ping Zhang is a Professor at BUPT. Prof. Zhang is the Director of Key Lab. of Universal Wireless Communication (BUPT) of Ministry of Education and currently leading the Wireless Technology Innovation (WTI) Institute. He is a member of IEEE and Vice Director of Sino-Germany Joint Software Institute. He is one of three draftsmen of National Key Program, Member of Experts and Consultants Committee of NSFC. His major research interests include cognitive radio network, wireless communication theory and signal processing.